C. R. Chimie 19 (2016) 1625–1630

Contents lists available at ScienceDirect

Comptes Rendus Chimie

www.sciencedirect.com

Full paper/Mémoire

Analysis of hydroxyapatite crystallites in subchondral bone by Fourier transform infrared spectroscopy and powder neutron diffraction methods

Analyse des cristaux d'hydroxyapatite dans l'os sous chondral par spectroscopie infrarouge à transformée de Fourier et diffraction neutronique sur poudres

Christine Chappard [a, *], Gilles André [b], Michel Daudon [c], Dominique Bazin [d]

[a] *B2OA, UMR 7052 CNRS–Université Paris-Diderot PRES Sorbonne Paris Cité, 10, avenue de Verdun 75010 Paris, France*
[b] *Laboratoire Leon-Brillouin, (CEA–CNRS) Saclay, Gif-sur-Yvette Cedex 91191, France*
[c] *Laboratoire des lithiases, Service d'explorations fonctionnelles, Hôpital Tenon, 4, rue de la Chine, 75970 Paris cedex 20, France; UMRS 1155, Inserm UPMC Paris, France*
[d] *Laboratoire de chimie de la matière condensée de Paris UPMC, Collège de France, Paris, France*

ARTICLE INFO

Article history:
Received 18 November 2014
Accepted 26 March 2015
Available online 20 February 2016

Keywords:
FTIR
Powder neutron diffraction
Bone
Osteoarthritis
Hydroxy-apatite cristals
Anisotropy
Human tissues

Mots-clés :
Spectroscopie infrarouge à transformée de Fourier
Diffraction neutronique sur poudres
Ostéoarthrose
Cristaux d'hydroxyapatite
Anisotropie
Corps humain

ABSTRACT

Fourier Transform Infrared (FTIR) spectroscopy and powder neutron diffraction (PND) were performed in human subchondral bone covered (C+) or not covered by cartilage (C−) to study hydroxyapatite. With FTIR, the carbonation rate was 30% with identical spectra in C+ and C−. With PND, the width of the diffraction peak (hkl = 002) highlighted the anisotropy of nanocrystals (with needle and/or platelet-like shape) along the c-axis with average length of 50 nm and thickness of 10 nm and with no difference between C+ and C−.

RÉSUMÉ

Des expérimentations par spectroscopie infrarouge à transformée de Fourier (FTIR) et par diffraction neutronique sur poudres (PND) ont été réalisées sur de l'os sous-chondral humain recouvert (C+) ou non recouvert par le cartilage (C) pour étudier l'hydroxyapatite (HAP).
En FTIR, le taux de carbonatation est de 30% avec des spectres identiques pour C+ et C−. Avec la PND, la largeur du pic de diffraction (hkl = 002) a mis en évidence l'anisotropie des nanocristaux (en forme aiguille et/ou de plaquettes) le long de l'axe c, avec une longueur moyenne de 50 nm et une épaisseur de 10 nm, sans différence entre C+ et C−.

* Corresponding author. B2OA, UMR 7052 CNRS- Université Paris Diderot, 10 avenue de Verdun 75010 Paris, France.
E-mail addresses: christine.chappard@inserm.fr (C. Chappard), gilles.andre@cea.fr (G. André), michel.daudon@tnn.aphp.fr (M. Daudon), dominique.bazin@upmc.fr (D. Bazin).

http://dx.doi.org/10.1016/j.crci.2015.03.015

1. Introduction

Osteoarthritis (OA) is characterized by the progressive destruction of articular cartilage and by changes in subchondral bone [1–3]. Radiographic evidence of hip OA is present in 5% of the population over the age of 65 years [4]. Sclerosis of the subchondral bone is regarded as one of the major radiologic features of OA [5]. There are strong interactions between the subchondral bone (beneath the cartilage) and cartilage. Indeed, it has been suggested that repetitive impact loading induces subchondral bone changes, resulting in a less compliant trabecular bone, which then transfers excessive mechanical stress to the overlying articular cartilage [6]. In a previous study, hip OA specimens were imaged by microcomputed tomography using synchrotron radiation (resolution = 10 μm). Substantial morphological, connectivity and anisotropy changes in the subchondral bone of advanced OA were demonstrated when cartilage was missing compared with adjacent areas covered by normal cartilage [7]. Moreover, when the cartilage is normal, the microarchitecture characteristics of the underlying subchondral bone have been found to be close to those from the subchondral bone of the femoral head in patients with hip fracture [7]. In the same study, the degree-of-mineralization (based on gray level calibration from X-rays extracted from the synchrotron radiation) has been shown decreased in the subchondral areas where cartilage was lacking compared with adjacent areas covered by normal cartilage [7].

Bone is a complex composite [8–13], and it is a natural fiber-reinforced material. The apatite crystals considerably increase the strength and the stiffness of the material, and this chemical composition could change with age and maturity and in some pathological conditions [14]. Recently significant breakthroughs have been obtained regarding the intimate structure of bone [15–18]. For example, E. Davies et al. [19] have assessed the incorporation of citrate between mineral platelets. The peculiar localization of this small molecule can explain the flat, plate-like morphology of bone mineral platelets and may be important in controlling the crystallinity of bone mineral, which in turn, is highly relevant to the mechanical properties of bone.

Different approaches are available to study physiological and pathological calcifications which are generally both made of an intimate mixing of mineral and organic parts with a hierarchical structure [20–25]: direct morphological measurements using a microscopy approach, vibrational methods and diffraction methods. Finally, technics specific to large scale instruments such as X-ray absorption spectroscopy [26,27] can be used also in order to probe the local order around Ca [28–34] or trace elements such as Zn [35–40], Pb [41] or Sr [42–46].

Transmission electron microscope (TEM) [47–49] of dispersed crystals was found to involve direct measurement of crystal lengths and widths, but not thicknesses [50]. Atomic force microscopy (AFM) [51–53] was also used to assess the crystal size and morphology on bovine powdered bone samples [54]. Vibrational methods, are represented by Raman spectroscopy [55–58], Fourier transform infrared (FTIR) spectroscopy [59–63], and the derived imaging method (FTIR-I). In the FTIR spectrum, it was possible to examine the molecular structure and conformation of biological macromolecules because FTIR spectroscopy measures the absorption energy, which produced an increase in the vibrational and rotational energy of atoms or groups of atoms within a molecule [64–70]. The wavelengths of many IR absorption bands were characteristic of specific types of chemical bonds. The shifts in band intensities and positions were caused by changes in the environment of the molecule, enabling variations in these environments to be detected [71]. The IR spectrum of bone showed the presence of the major molecular species, including phosphate (from the mineral hydroxyapatite) and carbonate (from carbonate substitution for hydroxyl and phosphate groups in hydroxyapatite) [71]. The FTIR method has been widely used to study bone fragility in osteoporosis [71]. In contrast, OA subchondral bone from the knee joint has been studied only one time in humans and was compared with normal trabecular bone harvested at the tibia [72].

The mostly used diffraction method is X-ray diffraction (XRD) and more rarely powder neutron diffraction (PND) [73–79], when small-angle instrument are used for detection, the technique is called: small-angle scattering either by X-rays (SAXS) or by neutrons (SANS). With diffraction methods, the position and the intensity of the peaks are related to the spatial arrangement of the atoms and to the atomic weight. SAXS is sensitive to the electron density contrast between the mineral matrix and the organic matrix, and it provides information on the thickness, shape and orientation of the mineral crystals represented in bone by hydroxyapatite (HAP), $Ca_{10}(PO_4)_6(OH)_2$ [80–83]. This technique was previously used to study mineral particle thickness in mineralized cartilage and adjacent bone [84,85] and in OA [86]. X-ray diffraction on powdered bone was used one time to compare bone from femoral heads of patients with OA or osteoporosis [87].

Neutron diffraction has been previously employed to study bovine cortical bone [88] and human anorganic cancellous bone [89]. In the long bone of humans, the c-axes of the hexagonal HAP crystals are preferentially oriented in the directions of the stresses [90], which coincides with the longitudinal fiber direction. SANS analysis has been used one time in hydrated bone to measure the spacing between collagen molecules in OA and osteoporosis (OP) specimens [91]. Neutrons interact with nuclei and yield information similar to SAXS results, but with a great sensitivity to light elements (H, C, O, and N) [79]. Neutron beams are very penetrating and non-destructive. The great penetrating power permits up to 1 cm sections of bone to be examined. To our knowledge, there are no data available about the qualitative changes of HAP crystals in the OA subchondral bone as assessed by PND.

The aim of this study was to evaluate HAP changes in subchondral trabecular bone from human femoral heads in relation to OA without homogenizing the bone samples. For this purpose, from the same individuals, areas with full thickness loss of the cartilage (considered to be as the latest stage of the disease) were compared with subchondral trabecular bone in areas surrounded by the normal

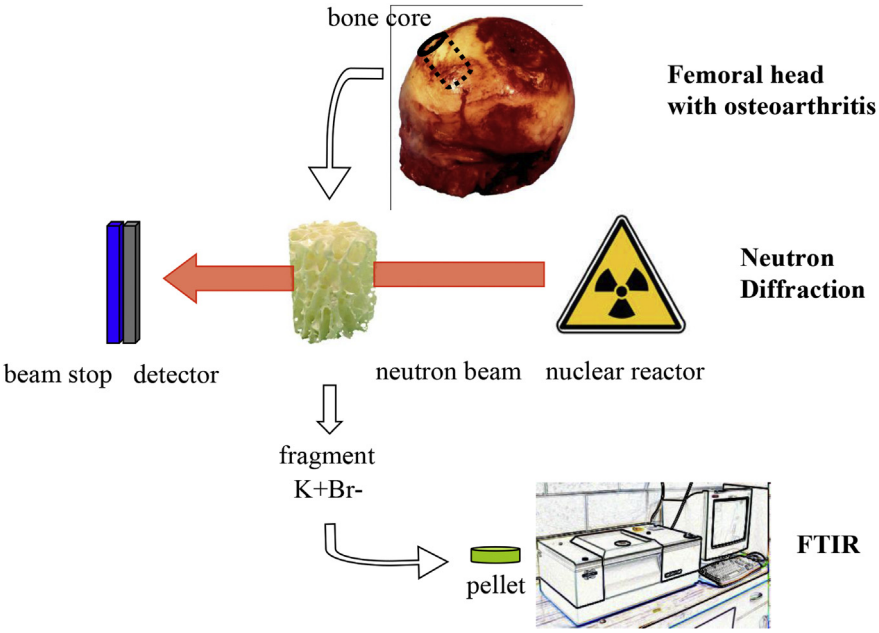

Fig. 1. Details of the experimental setup for the Fourier transform infrared spectroscopy analysis and the neutron diffraction experiment.

cartilage (considered to be normal bone). For that, the following techniques were using: FTIR spectroscopy and PND.

2. Materials and methods

The subchondral bone specimens were harvested from femoral heads removed during arthroplasty in 4 OA cases in females patients (orthopedic surgery department of Centre Hospitalier d'Orléans) (mean age: 73 ± 9 years). The ethical approval for collection of the samples was given by the Human Ethics Committee of Inserm. These patients had no evidence of congenital or acquired dysplasia or avascular necrosis and no obvious history of bisphosphonate or fluoride use. In each "osteoarthritic" femoral head, 2 subchondral bone cores were obtained: one without cartilage (C−) and the other covered with normal cartilage (C+) and located at the inferior pole. Cylindrical cores of subchondral bone 10 mm in height and 7 mm in diameter were prepared using a precision diamond trephine. All of the samples were harvested perpendicularly to the surface (consequently, perpendicular to the compressive stress) and included the subchondral trabecular bone immediately under the cartilage and the subchondral cortical bone layer. They were chemically defatted (one cycle of submerging in diluted bleach (3.6°) and several cycles in dichloromethane) in order to remove the bone marrow and fat rich in hydrogen, which lower the neutron signal-to-noise ratio.

For FTIR spectroscopy, fragments of the sample were the crushed particles sieved before making the, KBr pellets and analyzed with a Brucker® IFS25 spectrometer as previously described [92]. Data were collected in the absorption mode between 4000 and 400 cm^{-1} with a resolution of 4 cm^{-1}. The carbonate ratio (CR) of HAP was defined as the ratio between the intensity of the $\nu_2\nu_3$ bands of carbonate ions at 870 cm^{-1} and 1420 cm^{-1}, respectively, and the intensity of the $\nu_3\nu_4$ bands of phosphate ions at 1035 cm^{-1} and 604 cm^{-1}, respectively.

The neutron diffraction diagrams were collected on the G4.1 two-axis multidetector powder diffractometer [93] installed on a cold-source beamline of the Orphée reactor (Saclay, France). This beamline was equipped with a two-axis powder diffractometer, with a vertical-focusing pyrolytic graphite monochromator and an 800-cell multidetector covering an 80° 2θ range (step 0.1° between 2 cells). Neutron diffraction patterns were collected at room temperature between 7 and 87° using a wavelength of 2.4226 Å, with an acquisition time of a few hours, depending on the samples. The entire cylindrical sample was studied. This particular experimental setup offered the opportunity to determine the average size of nanocrystals in the range between 5 and 200 nm with the experimental protocol presented in (Fig. 1). The mean size of the crystals for each sample was calculated using the FullProf program [94,95].

3. Results

The carbonation rate was 30% with identical spectra in subchondral bone in C− and C+. The intensity of the signal was less pronounced in samples without cartilage compared with samples covered by cartilage from the same individual with typical FTIR spectra shown in (Fig. 2). The crystals were nanometer sized and the width of the diffraction peak ($hkl = 002$) was smaller than the width of the other diffraction peaks, highlighting the anisotropy of the nanocrystals of all of these compounds (needle and/or platelet-like morphology) along the *c*-axis. The average

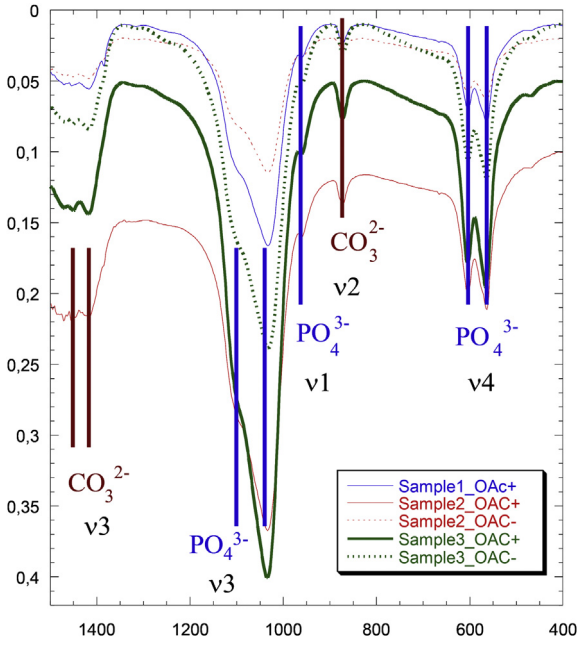

Fig. 2. Fourier transform infrared spectra of bones, with the contributions of PO_4^{3-} and CO_3^{2-} pointed out. Samples with cartilage are solid lines (OAC+), and samples without cartilage are dotted lines (OAC−).

length of the crystals was 50 nm, and the average thickness was 10 nm. There were no differences in the diffraction patterns between C− and C+ areas with typical diffraction patterns shown in (Fig. 3).

4. Discussion

The present study demonstrated that the crystal morphology and carbonate ratios of HAP in subchondral bone were not modified by the overlying cartilage alteration in OA. The average length of the crystal plates found in this study (50 nm) was the same as that found in literature by various techniques [96]. The thicknesses of mineralites (10 nm) were considered as being small mineralites [14]. FTIR methods are easy to employ and are the most frequently used. In contrast, PND was rarely used because it requires a nuclear reactor.

With the FTIR method, in all cases, the signal intensity was less pronounced in samples without cartilage compared with samples covered by cartilage from the same individuals, probably due to a lower quantity of mineral in region not covered by cartilage. These results are in accordance with our previous results: the local mineralization has been measured with monochromatic X-rays extracted from the synchrotron radiation and has been found to be decreased in areas without cartilage, which is related to a high remodeling rate [7]. The KBr technique has the advantage of being very simple; however, it is not possible to study the spatial arrangement of the sample as is possible with FTIR-I [71]. The absorbance bands for the vibration of protein amide bonds (Amide I, Amide II, Amide III) were not assessed because their IR spectra are usually concentrated in a very narrow range from 1200 to 1700 cm^{-1}. Moreover, the absorbance signal from protein is very low compared with phosphates. The large spectrum range that we covered was between 500 cm^{-1} and 1400 cm^{-1} with a 4 cm^{-1} resolution and does not allow this specific analysis. The most interesting part that it is shown in the Fig. 2 ranges from 2000 to 700 cm^{-1}, the section from 2000 to 4000 cm^{-1} presents low signal to noise ratio and consequently is less contributory even for proteins.

Using the SANS method, Skakle et al. used defatted bone from human femoral heads in OA and osteoporotic (OP) patients and one sample from the tibial cortex [91]. While the compressive trabecule were positioned vertically in the beam, the intensity of the peaks was less pronounced in trabecular bone than that in cortical bone. The authors interpreted this result as the possibility that the

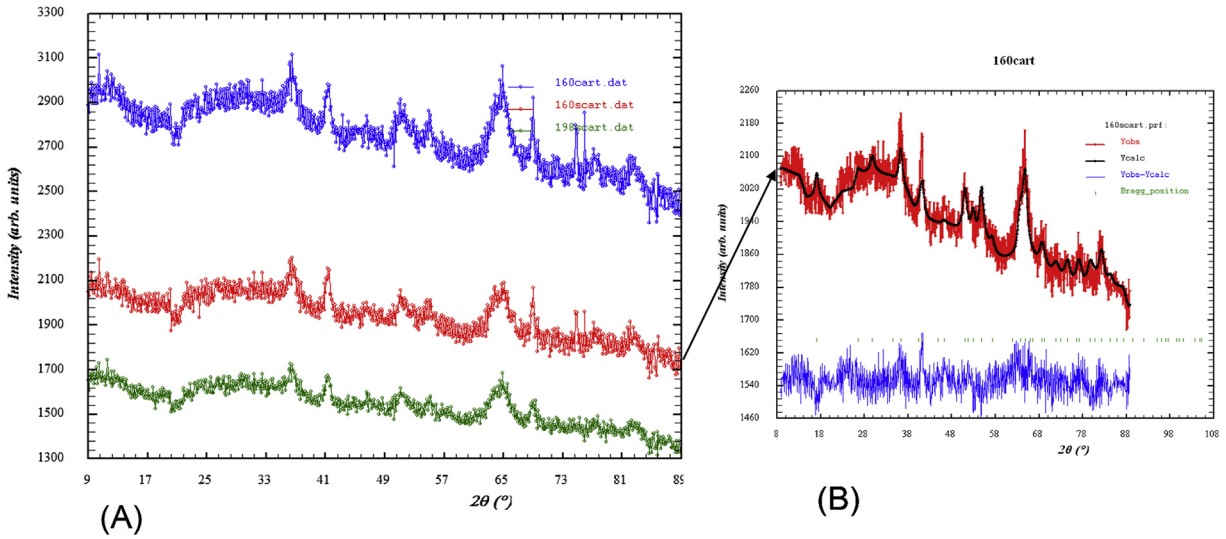

Fig. 3. Neutron diffraction diagrams. (A) The blue diagram corresponds to subchondral bone surrounded by cartilage, and the red and green diagrams correspond to subchondral bone without cartilage. (B) Diffraction model of the red diagram.

longitudinal alignment of collagen fiber is less marked in trabecular bone compared with cortical bone [91]. They described also lateral spacing of collagen fibers alignment in trabecular bone between 12.53 Å for OA specimens and 12.33 Å for OP specimens [91]. Using scanning SAXS, Zizak et al. showed that the mineral particle thickness in mineralized cartilage did not differ from bone and that mineral particles were oriented perpendicularly to the interface in the mineralized cartilage and paralleled the main collagen orientation in bone [84]. The crystallite size of the mineral was measured using X-ray diffraction in femoral head samples from OP and OA people, and no difference was observed [87].

Using both vibrational and diffraction methods, Camacho et al. found that with bone maturation, the crystal thickness increased and the crystals were better aligned, had less surface carbonate, and had more carbonate substituted for hydroxyl groups [82]. Moreover, in trabecular bone, HAP crystals were larger and were oriented to a larger degree than in cortical bone [82].

In normal human cortical and trabecular bone, the crystal size had dimensions ranging from 5 to 60 nm. The crystallites became larger with age, and larger crystals tended to reduce the stiffness of the bone [14]. However, the crystal size could depend on the sample preparation rather than the pathology itself [14]. In the present study, the only difference between samples was the presence or not of cartilage; consequently, the sample preparation could not influence the crystal size.

The main advantage of PND is the minimal sample preparation required due to the high penetration rate of neutrons, making it possible to explore the entire sample. For example, in Lui's study, to obtain SAXS results, they had to prepare 200-micron sections from embedded blocks [96]. We focused our measurements on a similar volume (1 cm in height) to that used in our previous study in which the microarchitectural changes of subchondral bone in the later stage of OA were described [7].

It may be interesting in future works to provide a more refined analysis based on the distance from the cartilage and to reduce the incoherent scattering in neutron diffraction. To do so, it would be necessary to remove all proteins.

5. Conclusion

The present study concludes that there are no ultrastructural changes in HAP in subchondral bone depending on the state of the underlying cartilage. The variations in biomechanical characteristics are probably mostly due to the microarchitectural and the degree-of-mineralization changes.

References

[1] N. Arden, M.C. Nevitt, Res. Clin. Rheumatol. 20 (2006) 3.
[2] D.J. Hunter, D.T. Felson, BMJ 332 (2006) 639.
[3] H.K. Ea, C. Nguyen, D. Bazin, A. Bianchi, J. Guicheux, P. Reboul, M. Daudon, F. Lioté, Arth. Rheum. 63 (2011) 10.
[4] N. Lane, N. Eng. J. Med. 357 (2007) 1413.
[5] D. Resnick, Diagnosis of bone and joints disorders, 4th ed., Philadelphia London Saunders, 2002.
[6] E.L. Radin, R.M. Rose, Clin. Orthop. 213 (1986) 34.
[7] C. Chappard, F. Peyrin, A. Bonassie, G. Lemineur, B. Brunet-Imbault, E. Lespessailles, C.L. Benhamou, Osteoarthr. Cartil. 14 (2006) 215.
[8] S. Mann, Nature 365 (1993) 499.
[9] S. Weiner, H.D. Wagner, Ann. Rev. Mater. Sci. 28 (1998) 271.
[10] M. Vallet-Regı, M.J. Gonzalez-Calbet, Prog. Solid State Chem. 32 (2004) 1.
[11] J.D. Currey, Science 309 (2005) 253.
[12] M.J. Glimcher, Rev. Mineral Geochem. 64 (2006) 223.
[13] P.Y. Chen, D. Toroian, P.A. Price, J. McKittrick, Calcif. Tissue Int. 88 (2011) 351.
[14] M.E. Ruppel, L.M. Miller, D.B. Burr, Osteoporos. Int. 19 (2008) 1251.
[15] Y. Wang, S. Von Euw, F.M. Fernandes, S. Cassaignon, M. Selmane, G. Laurent, G. Pehau-Arnaudet, C. Coelho, L. Bonhomme-Coury, M.-M. Giraud-Guille, F. Babonneau, Th Azaïs, N. Nassif, Nat. Mat 12 (2013) 1144.
[16] P. Fratzl, Nat. Mat 7 (2008) 610.
[17] D. Taylor, J.G. Hazenberg, T. Clive Lee, Nat. Mat 6 (2007) 263.
[18] F. Nudelman, K. Pieterse, A. George, P.H.H. Bomans, H. Friedrich, L.J. Brylka, P.A.J. Hilbers, G. de With, N.A.J.M. Sommerdijk, Nat. Mat 9 (2010) 1004.
[19] E. Davies, K.H. Müller, W.C. Wong, C.J. Pickard, D.G. Reid, J.N. Skepper, M.J. Duer, PNAS 111 (2014) E1354.
[20] S. Mann, J. Webb, R.J.P. Williams (Eds.), Biomineralisation: Chemical and Biochemical Perspectives, VCH Verlag, Weinheim, Germany, 1990.
[21] D. Bazin, M. Daudon, P. Chevallier, S. Rouziere, E. Elkaim, D. Thiaudiere, B. Fayard, E. Foy, Ann. Biol. Clin. 64 (2006) 125.
[22] E. Bauerlein (Ed.), Handbook of Biomineralization, Wiley-VCH Verlag GmbH & Co. KGaA, Weinheim, 2007.
[23] E. Bonucci, Biological Calcification, Normal and Pathological Processes in the Early Stages, Springer Verlag, Berlin, 2007.
[24] D. Bazin, M. Daudon, Ch. Combes, Ch. Rey, Chem. Rev. 112 (2012) 5092.
[25] Bazin, J.-Ph. Haymann, E. Letavernier, J. Rode, M. Daudon, La presse médicale 43 (2014) 135.
[26] D.E. Sayers, E.A. Stern, F.W. Lytle, Phys. Rev. Lett. 27 (1971) 1204.
[27] F.W. Lytle, D.E. Sayers, E.A. Stern, Phys. Rev. B 11 (1975) 4825.
[28] J.E. Harries, D.W.L. Hukins, S.S. Hasnain, Calcif. Tissue Inter 43 (1988) 250.
[29] F.E. Sowrey, L.J. Skipper, D.M. Pickup, K.O. Drake, Z. Lin, M.E. Smith, R.J. Newport, Phys. Chem. Chem. Phys. 6 (2004) 188.
[30] D. Laurencin, A. Wong, W. Chrzanowski, J.C. Knowles, D. Qiu, D.M. Pickup, R.J. Newport, Z. Gan, M.J. Duer, M.E. Smith, Phys. Chem. Chem. Phys. 12 (2009) 1081.
[31] Ch Nguyen, H.-K. Ea, D. Thiaudière, S. Reguer, D. Hannouche, M. Daudon, F. Lioté, D. Bazin, J. Synchrotron Rad 18 (2011) 475.
[32] J. Rajendran, S. Gialanella, P.B. Aswath, Mat Sci. Eng. C 33 (2013) 3968.
[33] J. Cosmidis, K. Benzerara, N. Nassif, T. Tyliszczak, F. Bourdelle, Acta Biomaterialia 12 (2015) 260.
[34] V. Martin-Diaconescu, M. Gennari, B. Gerey, E. Tsui, J. Kanady, R. Tran, J. Pécaut, D. Mag, V. Krewald, E. Gouré, C. Duboc, J. Yano, T. Agapie, M.-N. Collomb, S. DeBeer, Inorg. Chem. 54 (2015) 1283.
[35] Y. Tang, H.F. Chappell, M.T. Dove, R.J. Reeder, Y.J. Lee, Biomaterials 30 (2009) 2864.
[36] D. Bazin, X. Carpentier, I. Brocheriou, P. Dorfmuller, S. Aubert, C. Chappard, D. Thiaudière, S. Reguer, G. Waychunas, P. Jungers, M. Daudon, Biochimie 91 (2009) 1294.
[37] H. Murata, K. Shitara, I. Tanaka, A. Nakahira, T. Mizoguchi, K. Matsunaga, J. Phys. Condens. Matter 22 (2010) 384213.
[38] S. Gomes, J.M. Nedelec, E. Jallot, D. Sheptyakov, G. Renaudin, Chem. Mater. 23 (2011) 3072.
[39] A. Dessombz, Ch Nguyen, H.-K. Ea, S. Rouzière, E. Foy, D. Hannouche, S. Réguer, F.-E. Picca, D. Thiaudière, F. Lioté, M. Daudon, D. Bazin, J. Trace Elem. Med. Biol. 27 (2013) 326.
[40] S. Gomes, A. Kaur, J.-M. Nedelec, G. Renaudin, J. Mater. Chem. B 2 (2014) 536.
[41] F. Meirer, B. Pemmer, G. Pepponi, N. Zoeger, P. Wobrauschek, S. Sprio, A. Tampieri, J. Goettlicher, R. Steininger, S. Mangold, P. Roschger, A. Berzlanovich, J.G. Hofstaetter, C. Streli, J. Synchrotron Rad 18 (2011) 238.
[42] M. Korbas, E. Rokita, W. Meyer-Klaucke, J. Ryczek, J. Biol. Inorg. Chem. 9 (2004) 67.
[43] J. Terra, E.R. Dourado, J.G. Eon, D.E. Ellis, G. Gonzalez, A.M. Rossi, Phys. Chem. Chem. Phys. 11 (2009) 568.
[44] D. Bazin, M. Daudon, C. Chappard, J.J. Rehr, D. Thiaudière, S. Reguer, J. Synchrotron Rad. 18 (2011) 912.
[45] D. Bazin, A. Dessombz, C. Nguyen, H.K. Ea, F. Lioté, J. Rehr, C. Chappard, S. Rouzière, D. Thiaudière, S. Reguer, M. Daudon, J. Synchrotron Rad. 21 (2014) 136.

[46] C. Frankr, R. Grundahl, A. Christer, K. Stahl, Cal. Tissue Inter 94 (2014) 248.
[47] M.A. Rubin, I. Jasiuk, J. Taylor, J. Rubin, T. Ganey, R.P. Apkarian, Bone 33 (2003) 270.
[48] M.A. Rubin, I. Jasiuk, Micron 36 (2005) 653.
[49] A.L. Rossi, S. Moldovan, W. Querido, A. Rossi, J. Werckmannd, O. Ersen, M. Farina, Micron 56 (2014) 29.
[50] V. Ziv, S. Weiner, Connect Tissue Res. 30 (1994) 165.
[51] P. Milovanovic, J. Potocnik, D. Djonic, S. Nikolic, V. Zivkovic, M. Djuric, Z. Rakocevic, Exp. Gerontol. 47 (2012) 154.
[52] E. Lefèvre, C. Guivier-Curien, M. Pithioux, A. Charrier, Comput. Methods Biomech. Biomed. Engin 16 (2013) 337.
[53] Z. Xiong, E. Mairiaux, B. Walter, M. Faucher, L. Buchaillot, B. Legrand, Sensors (Basel) 14 (2014) 20667.
[54] S.J. Eppell, W. Tong, J.L. Katz, L. Kuhn, M.J. Glimcher, J. Orthop. Res. 19 (2001) 1027.
[55] G. Penel, G. Leroy, C. Rey, C. Bres, Calcif. Tissue Int. 63 (1998) 475.
[56] J.A. Timlin, A. Carden, M.D. Morris, R.M. Rajachar, D.H. Kohn, Anal. Chem. 72 (2000) 2229.
[57] M.D. Morris, S. Mandair, Clin. Orthop. Relat. Res. 469 (2011) 2160.
[58] H. Ding, J.S. Nyman, J.A. Sterling, A. Sterling, D.S. Perrien, A. Mahadevan-Jansen, X.H. Bi, J. Biomed. Opt. 19 (2014) 111606.
[59] C. Rey, B. Collins, T. Goehl, R.I. Dickson, M.J. Glimcher, Calcif Tissue Int. 45 (1989) 157.
[60] E.P. Paschalis, F. Betts, E. DiCarlo, R. Mendelsohn, A.L. Boskey, Calcif. Tissue Int. 61 (1997) 480.
[61] A.L. Boskey, R. Mendelsohn, Vibr Spectrosc. 38 (2005) 107.
[62] R. Bhowmik, K.S. Katti, D. Verma, D.R. Katti, Mater. Sci. Eng. C 27 (2007) 352.
[63] E.P. Paschalis, R. Mendelsohn, A.L. Boskey, Clin. Orthop. Relat. Res. 469 (2011) 2170.
[64] D. Nguyen Quy, M. Daudon, Infrared et Raman Spectra of Calculi, Elsevier, Paris, 1997.
[65] K. Potter, J.J. Butler, W.E. Horton, R.G. Spencer, Arthritis Rheum. 43 (2000) 1580.
[66] K. Potter, L.H. Kidder, I.W. Levin, E.N. Lewis, R.G. Spencer, Arthritis Rheum. 44 (2001) 846.
[67] S. Takada, A. Shibata, H. Yonezu, T. Yamada, M. Takahashi, A. Abbaspour, N. Yasui, J. Med. Invest. 51 (2004) 133.
[68] M. Kim, X. Bi, W.E. Horton, R.G. Spencer, N.P. Camacho, J. Biomed. Opt. 10 (2005) 031105.
[69] L.M. Miller, P. Dumas, Biochim. Biophys. Acta 1758 (2006) 846.
[70] D. Bazin, M. Daudon, Ann. de Biol. Clin. (2015) 517.
[71] A. Boskey, N.P. Camacho, Biomaterials 28 (2007) 2465.
[72] M. Ueno, A. Shibata, S. Yasui, K. Yasuda, K. Ohsaki, Cell. Mol. Biol. 49 (2003) 613.
[73] A. Guinier, X-ray Diffraction in Crystals, Imperfect Crystals and Amorphous Bodies, Dunod, Paris, 1956.
[74] G.E. Bacon, A.E. Goodship, J. Appl. Crystallogr 40 (2007) 349.
[75] D. Arcos, J. Rodríguez-Carvajal, M. Vallet-Regí, Phys. Rev. B Condens Matter 350 (2004) E607.
[76] D. Arcos, J. Rodríguez-Carvajal, M. Vallet-Regí, Solid State Sci. 6 (2004) 987.
[77] A. Cedola, M. Mastrogiacomo, S. Lagomarsino, R. Cancedda, C. Giannini, A. Guagliardi, M. Ladisa, M. Burghammer, F. Rustichelli, V. Komlev, Spectrochim Acta B 62 (2007) 642.
[78] H. Zhou, C. Burger, I. Sics, B.S. Hsiao, B. Chu, B. Graham, M.J. Glimcher, J. Appl. Crystallogr. 40 (2007) 666.
[79] D. Bazin, C. Chappard, C. Combes, X. Carpentier, S. Rouzière, G. André, G. Matzen, M. Allix, D. Thiaudière, S. Reguer, P. Jungers, M. Daudon, Osteoporos. Int. 20 (2009) 1065.
[80] S. Naray-Szabo, Z. Kristallogr Kristallgeom Kristallphys Kristallchem 75 (1930) 387.
[81] J.C. Elliott, Structure and Chemistry of the Apatites and Other Calcium Orthophosphates, Elsevier, Amsterdam, 1994.
[82] N.P. Camacho, S. Rinnerthaler, P. Paschalis, R. Mendelsohn, A. Boskey, P. Fratzl, Bone 25 (1999) 287.
[83] T.J. White, D. Zhi Li, Acta Crystallogr. B 59 (2003) 1.
[84] I. Zizak, P. Roschger, O. Paris, B.M. Misof, A. Berzlanovich, S. Bernstorff, H. Amenitsch, K. Klaushofer, P. Fratzl, J. Struct. Biol. 141 (2003) 208.
[85] Y. Zhang, F. Wang, H. Tan, G. Chen, L. Guo, L. Yang, Int. J. Med. Sci. 9 (2012) 353.
[86] W. Kaabar, O. Gundogdu, A. Laklouk, O. Bunk, F. Pfeiffer, M.J. Farquharson, D.A. Bradley, Appl. Radiat. Isot 68 (2010) 730.
[87] L.D. Mkukuma, C.T. Imrie, J.M. Skakle, D.W. Hukins, R.M. Aspden, Ann. Rheum. Dis. 64 (2005) 222.
[88] S. Lees, H.A. Mook, Calcif Tissue Int. 39 (1986) 291.
[89] G.E. Bacon, P.J. Bacon, R.K. Griffiths, J. Anat. 128 (1979) 277.
[90] G.E. Bacon, R.K. Griffiths, J. Anat. 143 (1985) 97.
[91] J.M.S. Skakle, R.M. Aspden, J. Appl. Crystallogr. 35 (2002) 506.
[92] L. Estepa, M. Daudon, Biospectroscopy 3 (197) 347.
[93] http://www-llb.cea.fr/spectros/pdf/g41-llb.pdf.
[94] J. Rodriguez-Carvajal, IUCr Comm. Powder Diffraction Newsl. 26 (2001) 12.
[95] J. Rodriguez-Carvajal, Physica B 192 (1993) 55.
[96] Y. Liu, I. Manjubala, H. Schell, D.R. Epari, P. Roschger, G.N. Duda, P. Fratzl, J. Bone Miner Res. 25 (2010) 2029.